Nuclear Inst. and Methods in Physics Research B 447 (2019) 30–33

Contents lists available at ScienceDirect

Nuclear Inst. and Methods in Physics Research B

journal homepage: www.elsevier.com/locate/nimb

Ion bombardment induced atom redistribution in amorphous targets: MD versus BCA

G. Hobler[a,*], D. Maciążek[b], Z. Postawa[b]

[a] Institute of Solid State Electronics, TU Wien, Gußhausstraße 25-25a, A-1040 Wien, Austria
[b] Institute of Physics, Jagiellonian University, ul. Lojasiewicza 11, 30348 Kraków, Poland

ARTICLE INFO

Keywords:
Spontaneous pattern formation
Atom redistribution
Binary collision approximation
Molecular dynamics

ABSTRACT

Atom redistribution is an important mechanism of ion bombardment induced spontaneous pattern formation in amorphous or amorphized targets. It may be characterized by either molecular dynamics (MD) simulations or by Monte Carlo (MC) simulations based on the binary collision approximation (BCA). In this work we analyze problems of the BCA approach in predicting atom redistribution by comparing MC and MD simulations of recoil events in amorphized Si. We find that the MC results critically depend on the displacement energy used, on the choice of the free flight paths and maximum impact parameters, and on the construction of the trajectories. Moreover, the net atom redistribution as determined by MD is significantly larger for recoils starting near the surface than for bulk recoils. The effect is not reproduced by the MC simulations.

1. Introduction

Spontaneous pattern formation by energetic ion beams has received significant impetus in recent years from progress in the understanding of its mechanisms [1–12]. An important contribution to the field is the so-called crater function formalism [2,7,12], which derives the coefficients of the equation of surface motion from the moments of a crater function. These moments can be calculated by molecular dynamics (MD) simulations or by Monte Carlo (MC) simulations based on the binary collision approximation (BCA).

The crater function moments have contributions from sputtering [13], atom redistribution within the target [14], and ion implantation [10,12]. Often, the effect of atom redistribution dominates or at least is an important contribution. It enters the formalism through its contribution to the first crater function moment

$$M_x^{(1)} = \Omega_{Si} \sum_{i=1}^{n} \Delta x_i. \quad (1)$$

Here, a Si target has been assumed and the contribution of relocated implanted ions has been neglected. Ω_{Si} denotes the atomic volume of Si, n the number of Si atoms redistributed within the target, and Δx_i their displacement component in the direction of the projection of the ion beam to the surface (x axis). The redistributive contribution to the first moment thus describes the net displacement of the target atoms in x direction.

The purpose of this paper is to analyze problems of the BCA approach in determining the sum of the displacements appearing in Eq. (1). Shortcomings of the BCA compared to MD with respect to atom redistribution have been pointed out before [15,16]. On the other hand, MC simulations using the BCA have successfully been used in combination with the crater function formalism [17,18]. The discrepancy is likely due to different parameters and implementations of the MC codes. In the present work we focus our attention on the roles of displacement energy, free flight path selection, and trajectory construction.

2. Methodology

We assess the qualtity of BCA implementations by comparison of MC and MD simulations of atom redistribution resulting from recoils starting with given energy E, direction with respect to the surface, and depth z below the surface (Fig. 1). For MD the choice of the initial atom configuration is critical. At fluences sufficient to produce patterns, Si is amorphized. A not well relaxed sample may lead to unrealistic displacements [4,16]. One approach therefore is to exercise particular care when relaxing the initial atom configuration [16]. We have alternatively used sequential ion impacts on an initially virgin target until a steady state has been reached [12]. We use the target from Ref. [12] which has been produced by 2 keV Kr impacts with an incidence angle of 60° on a Si cell with $x \times y \times z$ dimensions approximately equal to

* Corresponding author.
E-mail address: gerhard.hobler@tuwien.ac.at (G. Hobler).

https://doi.org/10.1016/j.nimb.2019.03.028
Received 15 August 2018; Accepted 15 March 2019

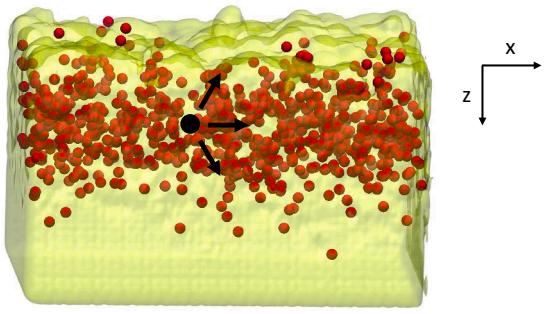

Fig. 1. Visual representation of the master sample used in the simulations of the recoil events. Si atoms are represented as a yellow transparent isosurface, Kr atoms as red spheres. A chosen primary recoil is represented by the black sphere.

150 Å × 100 Å × 100 Å, compare Fig. 1. The target contains a few percent of Kr atoms with a profile decaying towards the surface and the bulk. We assume their influence on the redistribution of Si atoms to be negligible. The target also exhibits surface roughness developed during the sequential impacts.

Simulations of the primary recoil events with energies between 5 eV and 100 eV are performed for three orientations of the velocity vector (Fig. 1), parallel to the x axis, at 60° pointing towards the surface, and at 60° pointing into the sample. For any given energy and orientation, 300 simulations are carried out where atoms with initial velocity are chosen randomly from a region 60 Å thick starting from the surface. Each simulation starts with a perfect copy of the master sample at 0 K temperature and is run for 1 ps. The applied boundary conditions and interatomic potentials are the same as in Ref. [12].

For the MC simulations we use the IMSIL code [19]. Unless otherwise noted we use the same models and parameters as in Ref. [12]. Unlike in [12], we neglect electronic stopping in order to allow a more consistent comparison with the MD results. In addition, we introduce variations into the BCA model as follows: First, in [12] the maximum impact parameter is chosen such that no collisions with energy transfer exceeding the displacement energy E_d are missed. This requires very large impact parameters p_{max} on the order of 3–4 Å at low recoil and displacement energies. The value of p_{max} is calculated from the minimum energy transfer and ion energy as proposed in [20]. The free flight path L is chosen according to

$$\pi p_{max}^2 L = \Omega_{Si} \quad (2)$$

in order to use the correct atomic density [21]. In contrast, often simply a constant free flight path of $L = \Omega_{Si}^{1/3}$ is used together with Eq. (2) [16,22]. For Si this leads to a fixed maximum impact parameter of $p_{max} = 1.53$ Å, which we consider as an option in our simulations.

Second, ion and recoil trajectories may be constructed in different ways. The most accurate treatment of a binary collision calculates the intersection point of the asymptotes using the "time integral" τ [23,24]. In Fig. 2 this point is denoted 1', and its distance from the foot of the impact parameter on the incoming asymptote is denoted x_1. Putting the ion at this point after a collision is the standard treatment in IMSIL, which we therefore label as "IMSIL default". Note that the initially chosen free flight path L is the distance between the ion (1) and the foot of the impact parameter on the incoming asymptote. The actual free flight path is reduced by x_1 to $ffp = L - x_1$ as shown in Fig. 2a.

At low energies, x_1 may be quite large [24], and at the same time the free flight paths L are small due to the energy transfer criterion. Therefore the actual free flight paths ffp may become negative, meaning that the ion is moved in the opposite direction of its momentum (cf. Fig. 2b). To avoid this unphysical situation, the free flight paths ffp were limited to non-negative values in Ref. [12]. We denote this model as "$ffp > 0$". It comes at the expense of unphysically shifting the outgoing asymptote in the forward direction.

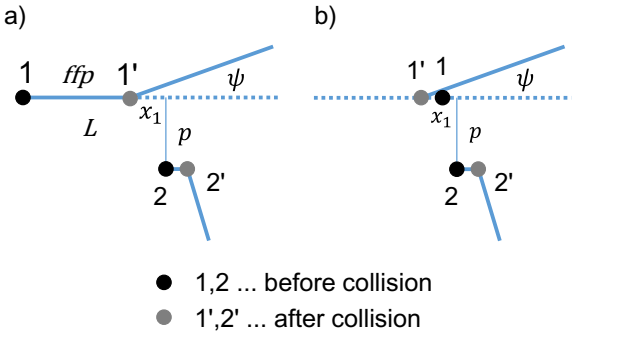

Fig. 2. Asymptotes of the ion (1) and recoil (2) trajectories. The ion is assumed to initially move to the right. In the standard model, after the collision, ion and recoil are placed into the intersection points of incoming and outgoing asymptotes. This normally leads to positive actual free flight paths ffp for a given chosen free flight path L (panel a), but can also lead to movement in the direction opposite to the initial ion momentum at low energies (panel b).

As a third option, the turning point of the ion trajectory may be assumed at the foot of the impact parameter on the incoming asymptote ($x_1 = 0$, which we will refer to as "no τ" or "TRIM") as is done in most MC codes for amorphous targets. This avoids the discrepancy between actual and chosen free flight path (ffp vs. L), again at the expense of constructing a wrong outgoing asymptote. The latter may seem as the lesser of the two evils. However, consider the case when the ion trajectory ends and the impact parameter p and the distance x_1 are large. Then the model which puts the ion at the intersection of the asymptotes terminates the trajectory considerably before the target atom (2), which is qualitatively correct. In contrast, the "no τ" model puts the ion close to atom 2, which is unphysical.

3. Results and discussion

3.1. Bulk simulations

In our recoil simulations we first only consider recoils starting at depths between 30 Å and 60 Å in order to exclude surface effects. A first set of results for recoils starting parallel to the surface is summarized in Fig. 3. In all panels the first moment according to Eq. (1) is shown as a function of the recoil energy. Results obtained with different BCA models (dashed lines) are compared to the MD results (black dots with error bars connected by black lines). Different displacement energies E_d are indicated by different colors. In the top row the energy dependent model for the maximum impact parameter is used which guarantees that no energy transfers above E_d are missed. With the default IMSIL model (left column) the MC simulations cannot be fitted to the MD data by varying the displacement energy; the best result is obtained with $E_d = 5$ eV. Oddly, the first moment can become negative for small displacement energies ($E_d = 1$ eV and $E_d = 0.25$ eV), i.e., the sum of the atom displacements is opposite to the direction of the initial recoil momentum, which is clearly unphysical. This does not happen when the actual free flight paths are restricted to non-negative values as described in Section 2 (middle column). Then a displacement energy of 5 eV yields an excellent fit to the MD data. With the TRIM model (right column) the problem of negative moments does not occur either, but an optimum fit is now obtained with a displacement energy near 15 eV. With the TRIM model the longest free flight paths are chosen among the three models, which is compensated for by a smaller number of recoils resulting from a larger displacement energy. In the bottom row of Fig. 3, the corresponding MC results using a fixed maximum impact parameter of 1.53 Å are shown. Now the MD data are well fitted with displacement energies near 15 eV.

Fig. 4 shows the displacement Δx_1 of the primary recoil in addition to the sum of all displacements for the three models with the best fit of

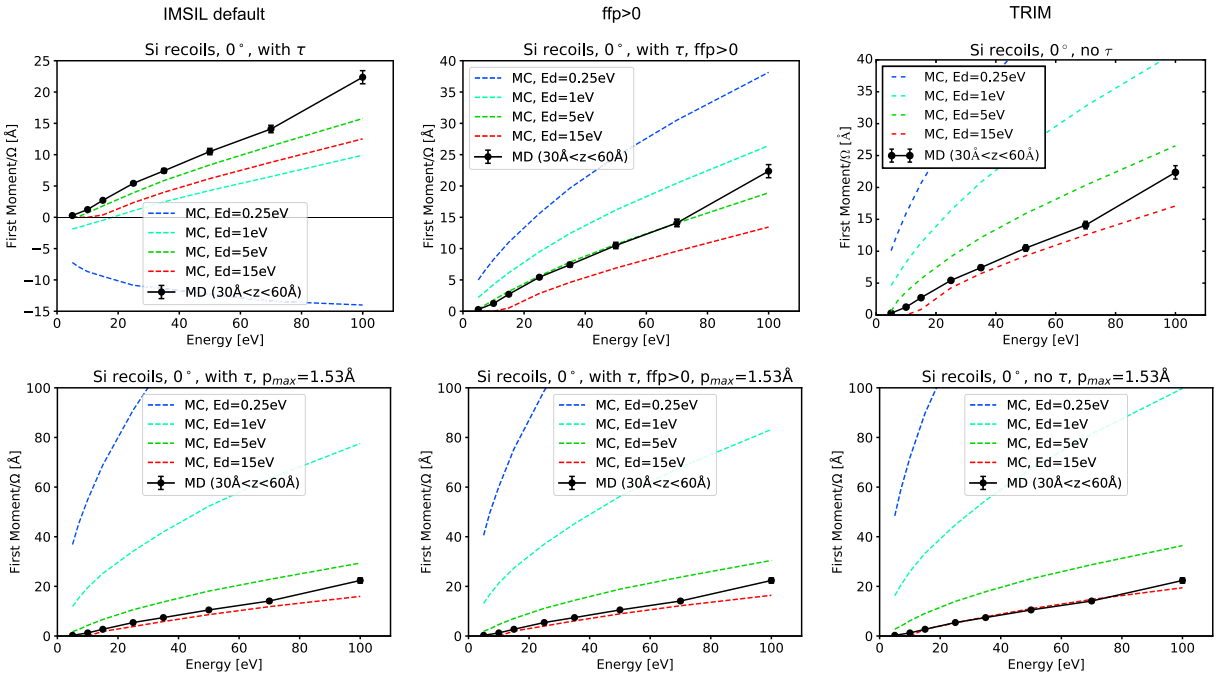

Fig. 3. First moment as a function of the recoil energy using various BCA models. Top row: using the energy dependent maximum impact parameter; bottom row: using a fixed maximum impact parameter of 1.53 Å. Columns 1–3: different trajectory construction models, see Section 2. The MD results represented by the black symbols with error bars, connected by lines, are the same in all panels. Recoils are started parallel to the surface.

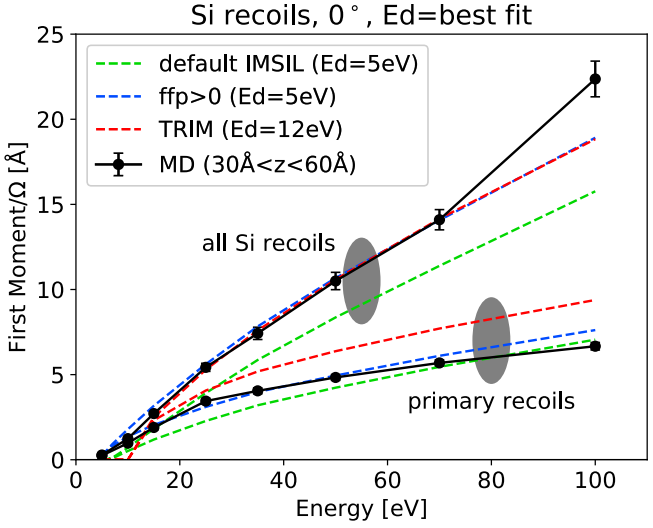

Fig. 4. First moment as a function of recoil energy. Symbols and lines have the same meaning as in Fig. 3. The displacement energy with the best fit to the MD data and the energy dependent maximum impact parameter model have been chosen for the MC simulations. In addition to the first moment the contribution of the primary recoil, i.e., the displacement of the primary recoil parallel to the surface, is shown.

the displacement energy. While both the *ffp* > 0 model and the TRIM model are in excellent agreement with the MD data taking all recoils into account, the TRIM model overestimates the displacement of the primary recoil. Since the displacement of the primary recoil is one term in the sum defining the first moment, Eq. (1), this is compensated for by fewer terms in the sum, which is accomplished by the higher displacement energy. Thus, the TRIM model partitions the first moment unphysically into contributions of the primary recoils and those of higher-order recoils. The *ffp* > 0 model therefore appears to be preferable.

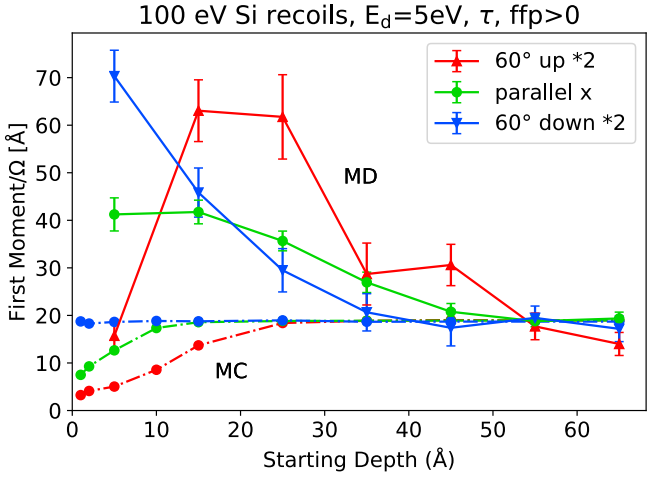

Fig. 5. First moment as a function of primary recoil depth z for 100 eV recoils starting parallel to the surface or at 60° with respect to the x axis towards or away from the surface. MD results collect data from [z–5 Å,z+5 Å]. MC simulations have used the *ffp* > 0 model. The results for the inclined initial recoil directions have been multiplied with two.

3.2. *The effect of the surface*

First moments resolved with respect to the starting depth of the primary recoils are shown in Fig. 5 for a recoil energy of 100 eV. Focussing first on recoils starting parallel to the surface (green lines), one observes a significant increase in the first moment towards the surface in case of the MD results, while the first moment calculated by MC decreases towards the surface. The decrease in the MC results is easily explained: Some recoils escape into the vacuum and cannot produce higher-order recoils there, thus reducing the number of terms in Eq. (1). The increase in the MD results indicates a reduced resistance of the surface atoms against relocation. As the effect is quite substantial, this reduced resistance likely extends to considerable depth, indicating collective motion of atoms in a near-surface layer of the target.

Fig. 5 also contains simulation results for recoils starting at 60° with respect to the x axis either towards the surface (red lines) or towards the bulk (blue lines). At large enough depths, under isotropic conditions the calculated first moments should be $\cos 60° = 1/2$ of the results for the initial direction parallel to the surface. The results for the inclined initial directions have therefore been multiplied with a factor of two. The good agreement of the results for the three initial conditions deeper in the sample indicates the absence of (artificial) anisotropies.

The first moments calculated by MD for primary recoils directed towards the surface (red lines) show a strong increase as a function of decreasing initial depth, until close to the surface where they are strongly lowered. A pronounced decrease towards the surface is also observed in the MC results. The larger decrease in both the MD and MC results, compared to when the primary recoils start parallel to the surface, is due to the fact that recoils have a larger probability of escaping into the vacuum when the primary recoil is directed towards the surface. The strong increase in the MD result at intermediate depths indicates that the collective motion is facilitated when a larger part of the recoil cascade is near the surface.

When the primary recoils are directed towards the bulk (blue lines), there is virtually no influence of the primary recoil depth on the first moment in the MC results, indicating that very few recoils escape into the vacuum even when the primary recoil starts at the surface. This is confirmed, e.g., by a MC sputtering yield of $Y = 0.1$ for primary recoils starting at a depth of 2 Å with a component into the bulk, compared to $Y = 1.05$ for the same primary recoils starting parallel to the surface. The MD results show a substantial increase towards the surface with a maximum at the surface that exceeds even the maximum for the recoils directed towards the surface.

4. Conclusions

We have shown that atom redistribution as calculated by MC simulations strongly depends on the implementation of the BCA, i.e., on the displacement energy, the choice of the free flight path and the maximum impact parameter, and the construction of the trajectories. To the knowledge of the authors, in all previous work targeted at predicting spontaneous pattern formation using MC simulations, these details have not completely been specified. This means that none of these publications is reproducible.

For recoils starting deep in the bulk, we have obtained best results by limiting the free flight paths to non-negative values and choosing a displacement energy of $E_d = 5$ eV. This value is considerably higher than the value used in our impact simulations [12]. For the impact simulations, the choice of $E_d = 5$ eV results in considerably underestimated contributions to the first moment. The reason is the surface effect described in Section 3.2: The target atoms are much more mobile near the surface, probably due to some collective motion. Modeling this surface effect is an important challenge, if realistic MC simulations are aspired.

Acknowledgments

DM and ZP gratefully acknowledge financial support from the Polish National Science Centre, Grant No. 2015/19/B/ST4/01892. MD simulations were performed at the PLGrid computer facilities.

References

[1] N. Kalyanasundaram, M. Ghazisaeidi, J.B. Freund, H.T. Johnson, Single impact crater functions for ion bombardment of silicon, Appl. Phys. Lett. 92 (13) (2008) 131909 .
[2] S.A. Norris, M.P. Brenner, M.J. Aziz, From crater functions to partial differential equations: a new approach to ion bombardment induced nonequilibrium pattern formation, J. Phys: Condens. Matter 21 (2009) 224017 .
[3] M.Z. Hossain, K. Das, J.B. Freund, H.T. Johnson, Ion impact crater asymmetry determines surface ripple orientation, Appl. Phys. Lett. 99 (15) (2011) 151913 .
[4] S.A. Norris, J. Samela, L. Bukonte, M. Backman, F. Djurabekova, K. Nordlund, C.S. Madi, M.P. Brenner, M.J. Aziz, Molecular dynamics of single-particle impacts predicts phase diagrams for large scale pattern formation, Nature Commun. 2 (2011) 276.
[5] P.D. Shipman, R.M. Bradley, Theory of nanoscale pattern formation induced by normal-incidence ion bombardment of binary compounds, Phys. Rev. B 84 (8) (2011) 085420, https://doi.org/10.1103/PhysRevB.84.085420.
[6] M. Castro, R. Gago, L. Vázquez, J. Muñoz García, R. Cuerno, Stress-induced solid flow drives surface nanopatterning of silicon by ion-beam irradiation, Phys. Rev. B 86 (21) (2012) 214107 .
[7] M.P. Harrison, R.M. Bradley, Crater function approach to ion-induced nanoscale pattern formation: craters for flat surfaces are insufficient, Phys. Rev. B 89 (24) (2014) 245401 .
[8] J. Muñoz García, L. Vázquez, M. Castro, R. Gago, A. Redondo-Cubero, A. Moreno-Barrado, R. Cuerno, Self-organized nanopatterning of silicon surfaces by ion beam sputtering, Mater. Sci. Eng. R: Reports 86 (2014) 1–44.
[9] D.A. Pearson, R.M. Bradley, Theory of terraced topographies produced by oblique-incidence ion bombardment of solid surfaces, J. Phys.: Condens. Matter 27 1 (2015) 015010, https://doi.org/10.1088/0953-8984/27/1/015010.
[10] R.M. Bradley, H. Hofsäss, Nanoscale patterns produced by self-sputtering of solid surfaces: The effect of ion implantation, J. Appl. Phys. 120 (7) (2016) 074302 .
[11] S.A. Norris, J.C. Perkinson, M. Mokhtarzadeh, E. Anzenberg, M.J. Aziz, K.F. Ludwig, Distinguishing physical mechanisms using GISAXS experiments and linear theory: the importance of high wavenumbers, Sci. Rep. 7 (1) (2017) 2016.
[12] G. Hobler, D. Maciążek, Z. Postawa, Crater function moments: role of implanted noble gas atoms, Phys. Rev. B 97 15 (2018) 155307, https://doi.org/10.1103/PhysRevB.97.155307.
[13] R.M. Bradley, J.M.E. Harper, Theory of ripple topography induced by ion bombardment, J. Vac. Sci. Technol. A 6 (4) (1988) 2390–2395.
[14] G. Carter, V. Vishnyakov, Roughening and ripple instabilities on ion-bombarded Si, Phys. Rev. B 54 (24) (1996) 17647–17653.
[15] L. Bukonte, F. Djurabekova, J. Samela, K. Nordlund, S. Norris, M. Aziz, Comparison of molecular dynamics and binary collision approximation simulations for atom displacement analysis, Nucl. Instrum. Meth. Phys. Res. B 297 (2013) 23–28, https://doi.org/10.1016/j.nimb.2012.12.014.
[16] A. Lopez-Cazalilla, A. Ilinov, L. Bukonte, K. Nordlund, F. Djurabekova, S. Norris, J.C. Perkinson, Simulation of redistributive and erosive effects in a-Si under Ar+ irradiation, Nucl. Instrum. Meth. Phys. Res. B 414 (2018) 133–140, https://doi.org/10.1016/j.nimb.2017.11.019.
[17] H. Hofsäss, Surface instability and pattern formation by ion-induced erosion and mass redistribution, Appl. Phys. A 114 (2) (2014) 401–422.
[18] H. Hofsäss, O. Bobes, K. Zhang, Argon ion beam induced surface pattern formation on Si, J. Appl. Phys. 119 (3) (2016) 035302 .
[19] G. Hobler, Monte Carlo simulation of two-dimensional implanted dopant distributions at mask edges, Nucl. Instrum. Meth. Phys. Res. B 96 (1995) 155.
[20] G. Hobler, A. Simionescu, Acceleration of binary collision simulations in crystalline targets using critical angles for ion channeling, Nucl. Instrum. Meth. Phys. Res. B 102 (1995) 24–28, https://doi.org/10.1016/0168-583X(94)00792-6.
[21] J.F. Ziegler, J.P. Biersack, U. Littmark, The Stopping and Range of Ions in Solids, Pergamon Press, New York, 1985.
[22] W. Möller, TRI3dyn – Collisional computer simulation of the dynamic evolution of 3-dimensional nanostructures under ion irradiation, Nucl. Instrum. Meth. Phys. Res. B 322 (2014) 23–33, https://doi.org/10.1016/j.nimb.2013.12.027.
[23] M.T. Robinson, I.M. Torrens, Computer simulation of atomic-displacement cascades in solids in the binary-collision approximation, Phys. Rev. B 9 (12) (1974) 5008–5024.
[24] W. Eckstein, Computer Simulation of Ion-solid Interactions, Springer, Berlin, 1991.